



# Ruthenium–tin complexes from the reaction of $\text{HSnPh}_3$ with $\text{Ru}_3(\text{CO})_{10}(\text{NCMe})_2$ and their reactions with bis(tri-*t*-butylphosphine)platinum

Richard D. Adams\*, Burjor Captain, Eszter Trufan

Department of Chemistry and Biochemistry, University of South Carolina, Columbia, SC 29208, United States

## ARTICLE INFO

### Article history:

Received 15 August 2008

Accepted 18 August 2008

Available online 2 September 2008

### Keywords:

Ruthenium carbonyl

Tin

Platinum

Mixed metal clusters

Triphenylstannane

## ABSTRACT

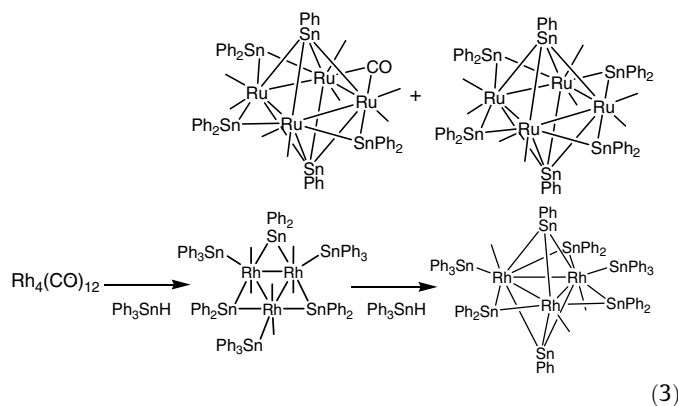
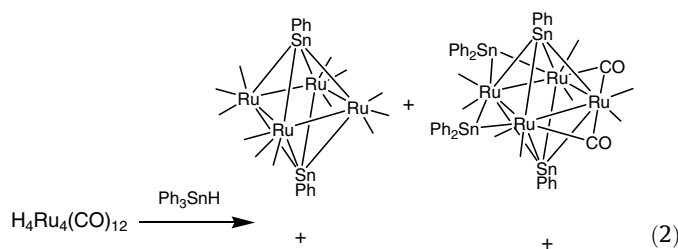
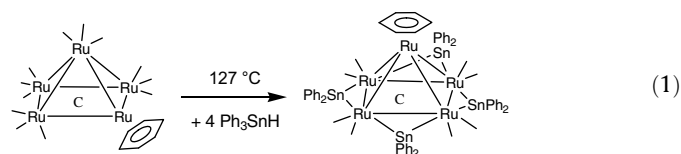
The compounds  $\text{Ru}_3(\text{CO})_9(\text{SnPh}_3)_2(\text{NCMe})(\mu\text{-H})_2$  (**1**),  $\text{Ru}_3(\text{CO})_{10}(\text{SnPh}_3)_2(\mu\text{-H})_2$  (**2**),  $\text{Ru}(\text{CO})_4(\text{SnPh}_3)_2$  (**3**) and  $\text{Ru}(\text{CO})_4(\text{SnPh}_3)(\text{H})$  (**4**) were obtained from the reaction of  $\text{Ru}_3(\text{CO})_{10}(\text{NCMe})_2$  with  $\text{HSnPh}_3$  in hexane solvent. Compounds **1**, **3** and the new compound  $\text{Ru}_3(\text{CO})_7(\text{SnPh}_3)_3(\text{NCMe})_2(\mu\text{-H})_3$  (**5**) were obtained from reaction of  $\text{Ru}_3(\text{CO})_{10}(\text{NCMe})_2$  with  $\text{HSnPh}_3$  in a  $\text{CH}_2\text{Cl}_2$  and MeCN solvent mixture. Compound **2** and the new compound  $\text{Ru}_3(\text{CO})_9(\text{SnPh}_3)_3(\mu\text{-H})_3$  (**6**) were obtained from reactions of **1** and **5** with CO, respectively. Compounds **2** and **6** eliminated benzene when heated to yield  $\text{Ru}_3(\text{CO})_{10}(\mu\text{-SnPh}_2)_2$  (**7**) and  $\text{Ru}_3(\text{CO})_9(\mu\text{-SnPh}_2)_3$  (**8**) which contain bridging  $\text{SnPh}_2$  ligands. Compound **7** was found to react with  $\text{Pt}(\text{PBU}_3)_2$  to yield the bis- $\text{Pt}(\text{PBU}_3)$  adduct,  $\text{Pt}_2\text{Ru}_3(\text{CO})_{10}(\text{PBU}_3)_2(\mu_3\text{-SnPh}_2)_2$  (**9**) in 59% yield by the addition of  $\text{Pt}(\text{PBU}_3)$  groups to two of the Ru–Sn bonds to the bridging  $\text{SnPh}_2$  ligands. Fenske–Hall molecular orbital calculations were performed to provide an understanding of the metal–metal bonding in the clusters of **7** and **9**. Compounds **1**, **2**, **5**, **6**, **7** and **9** were characterized structurally by single crystal X-ray diffraction analysis.

© 2008 Elsevier B.V. All rights reserved.

## 1. Introduction

It is well known that tin is an effective modifier of transition metal catalysts [1]. Recently, it has been shown that polynuclear metal carbonyl cluster complexes containing tin can serve as effective precursors to new families of multimetallic nanoscale catalysts that exhibit high activity and selectivity for certain types of hydrogenation reactions when they are deposited and activated on mesoporous silica supports [2–5].

We have shown that the tin-hydride compound  $\text{HSnPh}_3$  reacts readily with polynuclear metal carbonyl cluster complexes to yield a range of higher nuclearity metal cluster complexes having large numbers of tin-containing ligands, Eq. (1)–(3) [3,6,7]. Bridging tin ligands,  $\text{SnPh}_2$  [3,6–11],  $\text{SnPh}$  [3,7], and even naked Sn [10] are commonly formed by the cleavage of 1–3 of the Ph groups from the tin atom.



We have shown that  $\text{H}_2\text{SnPh}_2$  reacts with two equivalents of  $\text{Ru}(\text{CO})_5$  to give the  $\text{SnPh}_2$  bridged complex  $[\text{Ru}(\text{CO})_4\text{H}]_2(\mu\text{-SnPh}_2)$

\* Corresponding author.

E-mail address: Adams@mail.chem.sc.edu (R.D. Adams).



### 2.3. Reaction of $Ru_3(CO)_{10}(NCMe)_2$ with $HSnPh_3$ in $CH_2Cl_2/MeCN$

The reaction was done as follows: a 50 mg amount of  $Ru_3(CO)_{12}$  (0.078 mmol) was dissolved in 75 mL of  $CH_2Cl_2$ . To this solution 5 mL of MeCN was added and it was cooled to  $-78^\circ C$  in a dry ice/acetone bath. Then a suspension of 23 mg of  $Me_3NO \cdot 2H_2O$  in 2.5 mL of MeCN was added drop-wise. The cooling bath was then removed, and the solution was allowed to warm up to room temperature. The reaction was considered complete when the solution became yellow and the IR spectra showed the  $Ru_3(CO)_{10}(NCMe)_2$  as major product. At this point, the reaction-mixture was filtered over a silica gel column to remove the excess  $Me_3NO \cdot 2H_2O$ . To this solution a 110.5 mg amount of  $HSnPh_3$  (0.315 mmol) was added. After 20 min at room temperature the reaction was stopped and the solvent was removed in vacuo. The products were separated by TLC by using 4:1 hexane–methylene chloride solvent mixture to yield 6.8 mg of  $Ru_3(CO)_{12}$ , 12.5 mg of **3** (6% yield), 19.1 mg of **1** (19%) and 4.0 mg  $Ru_3(CO)_7(SnPh_3)_3(NCCH_3)_2(\mu-H)_3$  (**5**) (3% yield). Spectral data for **5**: IR  $\nu_{CO}$  ( $cm^{-1}$  in  $CH_2Cl_2$ ): 2086 (w), 2027 (vs), 2008 (s), 1964 (m).  $^1H$  NMR ( $CDCl_3$ , in ppm):  $\delta = 7.22$ – $7.75$  (m, 45H, Ph), 1.47 (s, 3H, Me), 1.43 (s, 3H, Me),  $-11.04$  (s, 1H, hydride,  $^2J_{119Sn-H} = 45.1$  Hz,  $^2J_{117Sn-H} = 40.5$  Hz),  $-12.55$  (s, 1H, hydride,  $^2J_{119Sn-H} = 32.4$  Hz,  $^2J_{117Sn-H} = 21.6$  Hz),  $-13.02$  (s, 1H, hydride,  $^2J_{119Sn-H} = 42.6$  Hz,  $^2J_{117Sn-H} = 13.5$  Hz). Elemental Anal. Calc.: C, 47.8; H, 3.33. Found: C, 48.1; H, 3.7%.

### 2.4. Reaction of **5** with CO

A 12.8 mg amount of **5** (0.0078 mmol) was dissolved in 25 mL benzene. This solution was purged with CO for 24 h at room temperature. The solvent was then removed in vacuo and the products separated by TLC by using 4:1 hexane–methylene chloride solvent mixture to yield 0.5 mg of yellow  $Ru_3(CO)_9(SnPh_3)_3(\mu-H)_3$  (**6**) (4%).

### 2.5. Reaction $Ru_3(CO)_{12}$ with $HSnPh_3$ under hydrogen

A 50 mg amount of  $Ru_3(CO)_{12}$  (0.078 mmol) was dissolved in 50 mL of heptane in a 100 mL three-neck flask. The solution was added a 98 mg amount of  $HSnPh_3$  (0.271 mmol) and heated to heptane reflux while  $H_2$  was bubbled through it. After 90 min, the reaction-mixture was cooled and the solvent was removed in vacuo. The products were separated by TLC by using 6:1 hexane–methylene chloride solvent mixture to yield 55.2 mg (44%) of  $Ru_3(CO)_9(SnPh_3)_3(\mu-H)_3$  (**6**). Other compounds resulting from this reaction are  $HRu(CO)_4SnPh_3$  (4.9 mg; 3.7%) [15]; the known compound  $Ru_3(CO)_9(\mu-SnPh_2)_3$  (**8**) (5.3 mg, 5% yield) [12], and traces of some yet uncharacterized compounds. Spectral data for **6**: IR  $\nu_{CO}$  ( $cm^{-1}$  in hexane): 2083 (m), 2041 (s), 2028 (m, sh).  $^1H$  NMR ( $CDCl_3$ , in ppm) at  $25^\circ C$ :  $\delta = 7.22$ – $7.759$  (m, 45H, Ph),  $-14.60$  (s, 3H, hydride). Elemental Anal. Calc.: C, 51.47; H, 3.29. Found: C, 51.07; H, 3.25%.

### 2.6. Reaction of **1** with CO

A 10.0 mg amount of **1** (0.0077 mmol) was dissolved in 15 mL hexane. The solution was then purged with CO for 2 h at room temperature. The solvent was removed in vacuo and the product was separated by TLC by using 4:1 hexane–methylene chloride solvent mixture to yield 2.0 mg of orange **2** (20%).

### 2.7. Transformation of **2** to $Ru_3(CO)_{10}(\mu-SnPh_2)_2$ (**7**)

A 12.6 mg amount of **2** (0.0098 mmol) was dissolved in 20 mL benzene and was refluxed for 30 min. The orange color of the solution darkened and IR spectra revealed the appearance of a new compound. The solvent was then removed in vacuo and the prod-

uct was separated by TLC by using 6:1 hexane–methylene chloride solvent mixture to yield 6.8 mg of orange **7** (61%). Spectral data for **7**: IR  $\nu_{CO}$  ( $cm^{-1}$  in  $CH_2Cl_2$ ): 2100 (m), 2064 (w), 2048 (m), 2029 (s), 1995 (m), 1864 (m).  $^1H$  NMR ( $CDCl_3$ , in ppm):  $\delta = 7.00$ – $7.71$  (m, 20 H, Ph). Mass Spec. EI/MS  $m/z$ : 1130,  $M^+$ ; 1073,  $M^+ - 2CO$ ; 990,  $M^+ - 5CO$ ; 934,  $M^+ - 7CO$ ; 848,  $M^+ - 10CO$ .

### 2.8. Thermal decomposition of **2** in an NMR tube

A 11.4 mg amount of **2** (0.0089 mmol) was dissolved in  $d_8$ -toluene and the solution was kept in an oil-bath at  $80^\circ C$  for 10 min.  $^1H$  NMR of the **2** was taken at the beginning and another  $^1H$  NMR was taken after the 10 min. The spectra revealed that the resonances corresponding to the hydrido ligands of **2** disappeared and new resonances corresponding to **7** and benzene (7.13 ppm) formed.

### 2.9. Transformation of **6** to $Ru_3(CO)_9(\mu-SnPh_2)_3$ (**8**)

A 7.4 mg amount of **6** (0.0046 mmol) was dissolved in 17 mL octane in a 100 mL three-neck flask. The solution was heated to reflux for 20 min. The reaction-mixture was cooled and the solvent was removed in vacuo. After work up, 5.4 mg of **8** (85% yield) was isolated. Compound **8** was reportedly obtained in a lower yield (20%) as product from the reaction of  $Ru_3(CO)_{12}$  with  $HSnPh_3$  at  $125^\circ C$  [12].

### 2.10. Reaction of **7** with $Pt(PBu_3)_2$

A 6.6 mg amount of **7** (0.0058 mmol) was dissolved in 13 mL  $CH_2Cl_2$ . To this solution a 7.3 mg amount of  $Pt(PBu_3)_2$  (0.0122 mmol) was added and stirred at room temperature for 65 min. The color of the solution turned dark purple and IR spectra showed the disappearance of the starting material. The solvent was then removed in vacuo and the product was isolated by TLC by using 4:1 hexane–methylene chloride solvent mixture to yield 6.6 mg of red  $Pt_2Ru_3(CO)_{10}(PBu_3)_2(\mu_3-SnPh_2)_2$  (**9**) (59%). Spectral data for **9**: IR  $\nu_{CO}$  ( $cm^{-1}$  in  $CH_2Cl_2$ ): 2079 (vw), 2031 (w), 2010 (s), 1973 (w), 1844 (m), 1717 (w).  $^1H$  NMR ( $CDCl_3$ , in ppm):  $\delta = 6.92$ – $7.86$  (m, 20 H, Ph), 1.21 (d, 18H, Me,  $^1J_{H-H} = 13.1$  Hz).  $^{31}P$  [ $^1H$ ] NMR ( $CDCl_3$ , in ppm) at  $25^\circ C$ :  $\delta = 109.77$  (s, 2P,  $^1J_{Pt-P} = 5822.3$  Hz). Mass Spec. ES/MS  $m/z$ : 1925,  $M^+ + H^+$ ; 1848,  $M^+ - Ph$ ; 1770,  $M^+ - 2Ph$ ; 1742,  $M^+ - 2Ph - CO$ .

### 2.11. Reaction of **1** with $Pt(PBu_3)_2$

A 23.5 mg amount of **1** (0.0181 mmol) was dissolved in 20 mL  $CH_2Cl_2$ . To this solution a 21.6 mg amount of  $Pt(PBu_3)_2$  (0.0361 mmol) was added. The solution was stirred at room temperature for 3 h. The solvent was removed in vacuo and the products were then separated by TLC using 4:1 hexane–methylene chloride solvent mixture to yield 2.0 mg of **9** (7%).

**Crystallographic analyses.** Orange single crystals of **1** suitable for X-ray diffraction analysis were obtained by slow evaporation of solvent from solutions in methylene chloride/hexane solvent mixtures at  $5^\circ C$ . Orange single crystals of **2** and **7** suitable for X-ray diffraction analysis were obtained by slow evaporation of solvent from solutions in methylene chloride/hexane solvent mixtures at room temperature. Yellow single crystals of **5** suitable for X-ray diffraction analysis were obtained by slow evaporation of solvent from solutions in methylene chloride/hexane solvent mixtures at  $-25^\circ C$ . The crystals of **6** were grown from a methylene chloride/hexane solvent mixture by cooling the solution to  $-25^\circ C$ . Dark red single crystals of **9** suitable for X-ray diffraction analysis were obtained by slow evaporation of solvent from a solution of methy-

lene chloride/pentane solvent mixtures at  $-25\text{ }^{\circ}\text{C}$ . Each data crystal was glued onto the end of a thin glass fiber. X-ray intensity data were measured by using a Bruker SMART APEX CCD-based diffractometer using Mo  $K\alpha$  radiation ( $\lambda = 0.71073\text{ \AA}$ ). The raw data frames were integrated with the SAINT+ program by using a narrow-frame integration algorithm [17]. Correction for Lorentz and polarization effects were also applied with SAINT+. An empirical absorption correction based on the multiple measurement of equivalent reflections was applied in each analysis by using the program SADABS. All structures were solved by a combination of direct methods and difference Fourier syntheses, and refined by full-matrix least-squares on  $F^2$ , using the SHELXTL software package [18]. All non-hydrogen atoms were refined with anisotropic thermal parameters. Hydrogen atoms were placed in geometrically idealized positions and included as standard riding atoms during the least-squares refinements. Crystal data, data collection parameters, and results of the refinements are listed in Table 1.

Compounds **1** and **7** crystallized in the triclinic crystal system. The space group  $P\bar{1}$  was assumed and confirmed by the successful refinement and solution of both structures. For compound **1** there are two formula equivalents of the complex in the asymmetric crystal unit. The asymmetric crystal unit of **7** contains only one formula equivalent of the complex.

Compound **2** crystallized in the orthorhombic crystal system. The space group  $Pbca$  was identified uniquely from the patterns of systematic absences observed in the intensity data. There is only one formula equivalent of the complex in the asymmetric crystal unit. Compounds **5** and **9** crystallized in the monoclinic crystal system. For **5** the systematic absences in the intensity data identified the unique space group  $P2_1/n$ . There is one formula equivalent of the complex present in the asymmetric unit. One formula equivalent of methylene chloride from the crystallization solvent also co-crystallized with the complex. This molecule was included in the analysis and was satisfactorily refined. For compound **9** the sys-

**Table 1**  
Crystallographic data for compounds **1**, **2**, **5**, **6**, **7** and **9**

Compound	<b>1</b>	<b>2</b>	<b>5</b>
Empirical formula	$\text{Ru}_3\text{Sn}_2\text{NO}_9\text{C}_{47}\text{H}_{35}$	$\text{Ru}_3\text{Sn}_2\text{O}_{10}\text{C}_{46}\text{H}_{33}$	$\text{Ru}_3\text{Sn}_3\text{N}_2\text{O}_7\text{C}_{65}\text{H}_{54} \cdot \text{CH}_2\text{Cl}_2$
Formula weight	1298.35	1286.31	1719.31
Crystal system	Triclinic	Orthorhombic	Monoclinic
Lattice parameters			
$a$ (Å)	13.5590(5)	18.4513(5)	10.1055(3)
$b$ (Å)	19.4162(8)	17.3186(4)	44.4974(13)
$c$ (Å)	20.5052(8)	29.1451(7)	14.7344(4)
$\alpha$ (°)	112.602(1)	90.00	90.00
$\beta$ (°)	94.531(1)	90.00	97.233(1)
$\gamma$ (°)	99.354(1)	90.00	90.00
$V$ (Å <sup>3</sup> )	4857.7(3)	9313.3(4)	6572.9(3)
Space group	$P\bar{1}$ (#2)	$Pbca$ (#61)	$P2_1/n$ (#14)
Z value	4	8	4
$\rho_{\text{calc}}$ (g/cm <sup>3</sup> )	1.775	1.835	1.737
$\mu$ (Mo $K\alpha$ ) (mm <sup>-1</sup> )	1.977	2.063	1.927
Temperature (K)	294(2)	294(2)	150(2)
$2\theta_{\text{max}}$ (°)	53.60	52.04	53.76
No. of observed reflections ( $I > 2\sigma(I)$ )	23700	9175	16384
No. of parameters	1135	558	762
Goodness-of-fit (GOF) <sup>a</sup>	1.002	1.029	1.122
Maximum shift in cycle	0.008	0.009	0.032
Residuals <sup>a</sup> : $R_1$ ; $wR_2$	0.0468, 0.0918	0.0426, 0.0791	0.0574, 0.1143
Absorption correction	Multi-scan	Multi-scan	Multi-scan
Maximum/minimum	1.000/0.613	1.000/0.774	1.000/0.751
Largest peak in final Difference map (e <sup>-</sup> /Å <sup>3</sup> )	1.289	0.829	1.353
	<b>6</b>	<b>7</b>	<b>9</b>
Empirical formula	$\text{Ru}_3\text{Sn}_3\text{O}_9\text{C}_{63}\text{H}_{47}$	$\text{Ru}_3\text{Sn}_2\text{O}_{10}\text{C}_{34}\text{H}_{20}$	$\text{Pt}_2\text{Ru}_3\text{Sn}_2\text{P}_2\text{O}_{10}\text{C}_{58}\text{H}_{74} \cdot 0.5\text{ C}_5\text{H}_{12}$
Formula weight	1607.29	1129.09	998.01
Crystal system	Trigonal	Triclinic	Monoclinic
Lattice parameters			
$a$ (Å)	25.0324(3)	8.8578(2)	19.8744(11)
$b$ (Å)	25.0324(3)	13.7920(4)	16.7622(9)
$c$ (Å)	17.0918(4)	16.2534(4)	21.9460(12)
$\alpha$ (°)	90	105.965(1)	90.00
$\beta$ (°)	90	98.231(1)	90.971(1)
$\gamma$ (°)	120	92.430(1)	90.00
$V$ (Å <sup>3</sup> )	9275.2(3)	1882.38(8)	7310.0(7)
Space group	$P\bar{3}$ (#147)	$P\bar{1}$ (#2)	$C2/c$ (#15)
Z value	6	2	4
$\rho_{\text{calc}}$ (g/cm <sup>3</sup> )	1.727	1.992	1.814
$\mu$ (Mo $K\alpha$ ) (mm <sup>-1</sup> )	1.960	2.536	5.180
Temperature (K)	294(2)	294(2)	294(2)
$2\theta_{\text{max}}$ (°)	50.06	56.66	53.78
No. of observed reflections ( $I > 2\sigma(I)$ )	8086	9328	7196
No. of parameters	593	442	370
Goodness-of-fit (GOF) <sup>a</sup>	1.031	1.016	1.058
Maximum shift in cycle	0.001	0.001	0.007
Residuals <sup>a</sup> : $R_1$ ; $wR_2$	0.0532; 0.1320	0.0363, 0.0785	0.0315, 0.0772
Absorption correction	Multi-scan	Multi-scan	Multi-scan
Maximum/minimum	1.00/0.86	1.000/0.832	1.000/0.589
Largest peak in final difference map (e <sup>-</sup> /Å <sup>3</sup> )	1.298	1.097	1.811

<sup>a</sup>  $R = \sum_{hkl} (|F_{\text{obs}}| - |F_{\text{calc}}|) / \sum_{hkl} |F_{\text{obs}}|$ ;  $R_w = [\sum_{hkl} w(|F_{\text{obs}}| - |F_{\text{calc}}|)^2 / \sum_{hkl} wF_{\text{obs}}^2]^{1/2}$ ,  $w = 1/\sigma^2(F_{\text{obs}})$ ;  $\text{GOF} = [\sum_{hkl} w(|F_{\text{obs}}| - |F_{\text{calc}}|)^2 / (n_{\text{data}} - n_{\text{vari}})]^{1/2}$ .

tematic absences in the intensity data were consistent with space groups  $Cc$  and  $C2/c$ . The latter was selected and confirmed by the successful solution and refinement of the structure. The molecule lies on a crystallographic twofold rotation axis. Also, one half formula equivalent of pentane from the crystallization solvent was cocrystallized with the complex. It was included in the analysis and satisfactorily refined.

Compound **6** crystallized in the trigonal crystal system. There were no systematic absences in the data. This is consistent with either of the space groups  $P3$  and  $P\bar{3}$ . The latter was subsequently confirmed by the successful solution and refinement of the structural analysis. There are three  $1/3$  molecules of **6** in the asymmetric crystal unit. Each lies on a threefold rotation site. For the molecule containing the atoms Ru(1) and Sn(1), all non-hydrogen atoms were refined with anisotropic thermal parameters. The hydride ligand was located and refined with a fixed isotropic thermal parameter. Hydrogen atoms on the phenyl rings were placed in geometrically idealized positions and included as standard riding atoms during the least-squares refinements. For the molecule which contains atoms Ru(1) and Sn(1), only the ruthenium, tin and the carbonyl group atoms could be refined with anisotropic thermal parameters. The carbon atoms on the phenyl rings are slightly disordered and were constrained by using the `SHELX FLAT` instruction and refined using isotropic thermal parameters. The hydride ligand was located and refined with a fixed isotropic thermal parameter. Hydrogen atoms on the phenyl rings were placed in geometrically idealized positions and included as standard riding atoms during the least-squares refinements. The third molecule was disordered over two orientations which were refined in the ratio 60/40. The two orientations are mirror images of each other. The  $Ru_3$  triangles in the two  $Ru_3Sn_3$  cores are offset by a rotation of  $45.51^\circ$  about their common  $C_3$  rotation axis. The disorder components in the entire molecule were located from the difference map and refined with fixed site-occupancy factors in the ratio 60/40. Only the ruthenium and tin atoms were refined with anisotropic thermal parameters. The hydride ligand was not located and not included in the refinement. Hydrogen atoms on the phenyl rings were placed in geometrically idealized positions and included as standard riding atoms during the least-squares refinements.

### 2.12. Molecular orbital calculations

All molecular orbital calculations reported herein were performed by using the Fenske–Hall (FH) method [19]. The calculations were performed by utilizing a graphical user interface developed [20] to build inputs and view outputs from stand-alone Fenske–Hall and MOPLOT2 binary executables [21]. Contracted double- $\zeta$  basis sets were used for the Ru 4d, Pt 5d, Sn 5p, P 3p, and C and O 2p atomic orbitals. The Fenske–Hall scheme is a non-empirical approximate method that is capable of calculating molecular orbitals for very large transition metal systems. For these calculations, the input structures were obtained from the positional parameters from the crystal structure analyses. The molecular structures are not optimized by these calculations. The *t*-butyl groups on the phosphine ligands and the phenyl groups on the  $SnPh_2$  ligands were replaced with hydrogen, e.g.  $PH_3$  and  $SnH_2$  to simplify the calculations.

## 3. Results

Two new compounds  $Ru_3(CO)_9(SnPh_3)_2(NCMe)(\mu-H)_2$  (**1**) (19% yield) and  $Ru_3(CO)_{10}(SnPh_3)_2(\mu-H)_2$  (**2**) were obtained from the reaction of  $Ru_3(CO)_{10}(NCMe)_2$  with  $H_2SnPh_3$  in hexane solvent at room temperature. Both compounds were characterized by a combination of IR,  $^1H$  NMR, mass spectra and by a single crystal X-ray diffraction analyses. There are two symmetry independent mole-

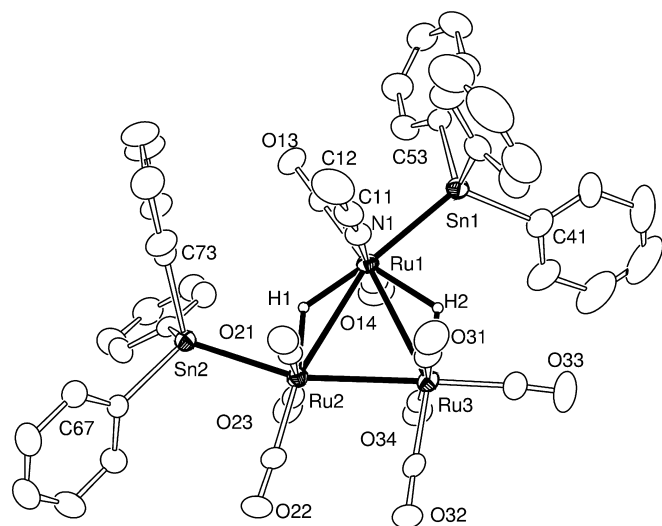


**Fig. 1.** An ORTEP diagram of the molecular structure of **1** showing 40% probability thermal ellipsoids. Selected bond distances (in Å) and angles ( $^\circ$ ) are as follows: (for molecule 1)  $Ru(1)-Ru(2) = 3.0844(6)$ ,  $Ru(1)-Ru(3) = 3.0797(7)$ ,  $Ru(2)-Ru(3) = 2.9144(6)$ ,  $Ru(1)-Sn(1) = 2.6773(6)$ ,  $Ru(2)-Sn(2) = 2.6488(6)$ ,  $Ru(1)-N(1) = 2.099(5)$ ,  $Ru(1)-H(1) = 1.76(6)$ ,  $Ru(1)-H(2) = 1.90(6)$ ,  $Ru(2)-H(1) = 1.69(7)$ ,  $Ru(3)-H(2) = 1.72(6)$ ; (for molecule 2)  $Ru(4)-Ru(5) = 3.0840(6)$ ,  $Ru(4)-Ru(6) = 3.0845(7)$ ,  $Ru(5)-Ru(6) = 2.9118(7)$ ,  $Ru(4)-Sn(3) = 2.6799(6)$ ,  $Ru(5)-Sn(4) = 2.6553(6)$ ,  $Ru(4)-N(2) = 2.116(5)$ ,  $Ru(4)-H(3) = 1.79(5)$ ,  $Ru(4)-H(4) = 1.69(5)$ ,  $Ru(5)-H(4) = 1.81(5)$ ,  $Ru(6)-H(3) = 1.80(5)$ .

cles in the crystal lattice of **1**. Both molecules are structurally similar. An ORTEP diagram of the molecular structure of one of these two molecules is shown in Fig. 1. Compound **1** contains a triangular cluster of three ruthenium atoms. There are two  $SnPh_3$  ligands and the tin atoms lie essentially in the plane of the  $Ru_3$  triangle. There are two bridging hydride ligands, nine terminal CO ligands and one MeCN ligand. The Ru–Sn bond distances,  $Ru(1)-Sn(1) = 2.6773(6)$  Å,  $Ru(2)-Sn(2) = 2.6488(6)$  Å [ $Ru(4)-Sn(3) = 2.6799(6)$  Å,  $Ru(5)-Sn(4) = 2.6553(6)$  Å], are slightly shorter than those found in the mononuclear ruthenium–tin compounds **3**, 2.7058(3) Å and 2.7121(3) Å [5] and **4**, 2.7108(3) Å [16]. The Ru–Ru bond distances are significantly longer than those found in  $Ru_3(CO)_{12}$ ,  $Ru-Ru = 2.854(1)$  Å [22]. The two longest Ru–Ru bonds in **1**,  $Ru(1)-Ru(2) = 3.0844(6)$  Å,  $Ru(1)-Ru(3) = 3.0797(7)$  Å, [ $Ru(4)-Ru(5) = 3.0840(6)$  Å,  $Ru(4)-Ru(6) = 3.0845(7)$  Å], contain bridging hydride ligands which are known to produce bond lengthening effects [23]. The other bond is much shorter  $Ru(2)-Ru(3) = 2.9144(6)$  Å [ $Ru(4)-Ru(5) = 2.9118(7)$  Å] and is only slightly longer than those in  $Ru_3(CO)_{12}$ . The hydride ligands were located and refined crystallographically and bridge the Ru–Ru bonds *cis* to the  $SnPh_3$  ligands,  $Ru(1)-H(1) = 1.76(6)$  Å,  $Ru(1)-H(2) = 1.90(6)$  Å,  $Ru(2)-H(1) = 1.69(7)$  Å,  $Ru(3)-H(2) = 1.72(6)$  Å [ $Ru(4)-H(3) = 1.79(5)$  Å,  $Ru(4)-H(4) = 1.69(5)$  Å,  $Ru(5)-H(4) = 1.81(5)$  Å,  $Ru(6)-H(3) = 1.80(5)$  Å]. The hydride ligands are inequivalent and the  $^1H$  NMR spectrum of **1** does exhibit two high-field resonances at  $\delta = -13.89$  (d, 1H,  $^2J_{H-H} = 1.8$  Hz),  $-15.04$  (d, 1H,  $^2J_{H-H} = 2.1$  Hz) with appropriate H–H coupling, as expected. The one MeCN ligand occupies an axial position on Ru(1) [ $Ru(4)$ ]:  $Ru(1)-N(1) = 2.099(5)$  Å,  $Ru(4)-N(2) = 2.116(5)$  Å. The one MeCN ligand shows its methyl resonance at  $\delta = 1.42$  (s, 3H) in the  $^1H$  NMR spectrum.

Compound **2** is structurally similar to **1** except that the MeCN ligand has been replaced by a terminally coordinated CO ligand (see Fig. 2). The Ru–Ru and Ru–Sn bond distances in **1** are similar to those in **2**. The two bridging hydride ligands are inequivalent as in **1**, and two high-field resonances were observed for these

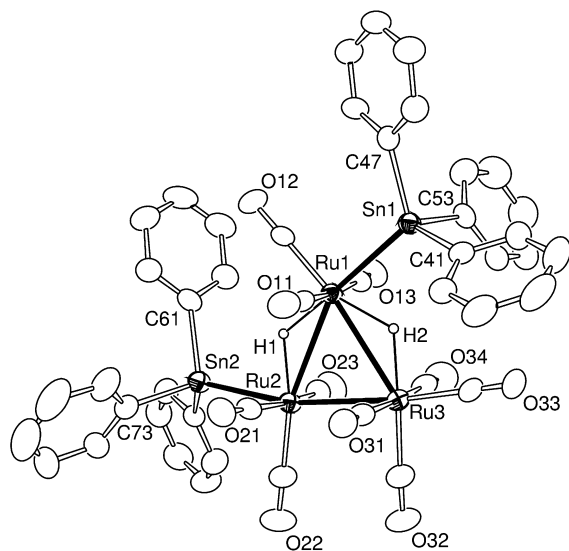


**Fig. 2.** An ORTEP diagram of the molecular structure of **2** showing 30% probability thermal ellipsoids. The hydrogen atoms are omitted for clarity. Selected interatomic bond distances (Å) and angles ( $^{\circ}$ ) are as follows: Ru(1)–Ru(2) = 3.0451(7), Ru(1)–Ru(3) = 3.0812(8), Ru(2)–Ru(3) = 2.9042(8), Ru(1)–Sn(1) = 2.6891(7), Ru(2)–Sn(2) = 2.6565(7), Ru(1)–H(1) = 1.74(7), Ru(1)–H(2) = 1.79(6), Ru(2)–H(1) = 1.75(7), Ru(3)–H(2) = 1.77(6); Sn(1)–Ru(1)–Ru(3) = 97.67(2), Sn(2)–Ru(2)–Ru(1) = 105.24(2).

ligands in the  $^1\text{H}$  NMR spectrum,  $\delta = -15.03$  (d, 1H,  $^2J_{\text{H-H}} = 0.7$  Hz),  $-16.68$  (d, 1H,  $^2J_{\text{H-H}} = 0.7$  Hz).

Compound **1** was also obtained in 19% yield from the reaction of  $\text{Ru}_3(\text{CO})_{10}(\text{NCMe})_2$  with  $\text{HSnPh}_3$  in a  $\text{CH}_2\text{Cl}_2/\text{MeCN}$  solvent mixture at room temperature. A small amount of **3** (6%) was also formed but there was none of the compounds **2** and **4**. Interestingly, however, a new compound  $\text{Ru}_3(\text{CO})_7(\text{SnPh}_3)_3(\text{NCMe})_2(\mu\text{-H})_3$  (**5**) was obtained in a low yield (3%). Compound **5** was characterized by a combination of IR,  $^1\text{H}$  NMR, elemental and a single crystal X-ray diffraction analyses. An ORTEP diagram of the molecular structure of **5** is shown in Fig. 3. The molecule contains a triangular cluster of three ruthenium atoms held together by three Ru–Ru bonds: Ru(1)–Ru(3) = 3.1284(6) Å, Ru(1)–Ru(2) = 3.1312(6) Å, Ru(2)–Ru(3) = 3.1329(6) Å. Each Ru–Ru bond also contains a bridging hydrido ligand. Bridging hydrido ligands are known to produce lengthening of the associated metal–metal bonds [23]. The hydrido ligands were located and refined crystallographically. The hydrido ligands lie in the plane of the  $\text{Ru}_3$  triangle: Ru(1)–H(1h) = 1.63(7) Å, Ru(1)–H(3h) = 1.86(9) Å, Ru(2)–H(1h) = 1.87(7) Å, Ru(2)–H(2h) = 1.84(7) Å, Ru(3)–H(2h) = 1.69(7) Å, Ru(3)–H(3h) = 1.61(9) Å. All three hydrido ligands are inequivalent and high-field resonances with appropriate Sn–H couplings were observed for them in the  $^1\text{H}$  NMR spectrum at  $\delta = -11.04$  (s, 1H,  $^2J_{119\text{Sn-H}} = 45.1$  Hz,  $^2J_{117\text{Sn-H}} = 40.5$  Hz),  $-12.55$  (s, 1H,  $^2J_{119\text{Sn-H}} = 32.4$  Hz,  $^2J_{117\text{Sn-H}} = 21.6$  Hz),  $-13.02$  (s, 1H,  $^2J_{119\text{Sn-H}} = 42.6$  Hz,  $^2J_{117\text{Sn-H}} = 13.5$  Hz). Each ruthenium atom contains one  $\text{SnPh}_3$  ligand. All three  $\text{SnPh}_3$  ligands lie in the plane of the  $\text{Ru}_3$  triangle. Ignoring the phenyl groups the other ligands the approximate symmetry is  $\text{C}_{3\text{h}}$ . The Ru–Sn bond distances, Ru(1)–Sn(1) = 2.6610(6) Å, Ru(2)–Sn(2) = 2.6681(6) Å, Ru(3)–Sn(3) = 2.6745(6) Å, are similar to those observed in **1** and **2**. Compound **5** contains seven linear terminal carbonyl ligands distributed as shown in Fig. 3 and two MeCN ligands. The latter occupy axial coordination sites on Ru(1) and Ru(2) cis to the  $\text{SnPh}_3$  ligands on opposite sides of the  $\text{Ru}_3$  plane: Ru(1)–N(1) = 2.093(5) Å and Ru(2)–N(2) = 2.112(7) Å. The MeCN ligands are inequivalent and two separate resonances are observed for their methyl groups in the  $^1\text{H}$  NMR spectrum:  $\delta = 1.47$  (s, 3H) and 1.43 (s, 3H).

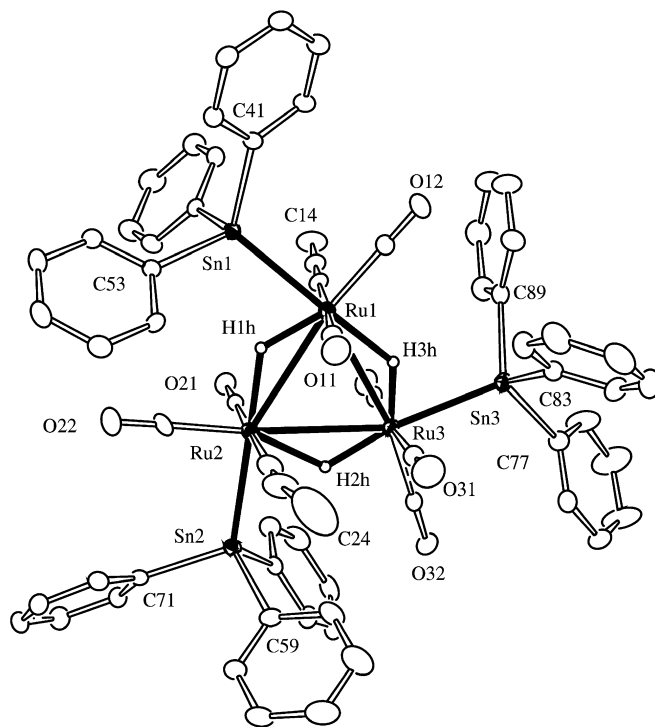


**Fig. 3.** An ORTEP diagram of the molecular structure of **5** showing 40% probability thermal ellipsoids. Selected bond distances (in Å) and angles ( $^{\circ}$ ) are as follows: Ru(1)–Ru(3) = 3.1284(6), Ru(1)–Ru(2) = 3.1312(6), Ru(2)–Ru(3) = 3.1329(6), Ru(1)–N(1) = 2.093(5), Ru(2)–N(2) = 2.112(7), Ru(1)–Sn(1) = 2.6610(6), Ru(2)–Sn(2) = 2.6681(6), Ru(3)–Sn(3) = 2.6745(6), Ru(1)–H(1h) = 1.63(7), Ru(1)–H(3h) = 1.86(9), Ru(2)–H(1h) = 1.87(7), Ru(2)–H(2h) = 1.84(7), Ru(3)–H(2h) = 1.69(7), Ru(3)–H(3h) = 1.61(9).

Compounds **1** and **5** both react with CO (1 atm/25  $^{\circ}\text{C}$ ) by substitution of their MeCN ligands to yield the fully carbonylated compounds  $\text{Ru}_3(\text{CO})_{10}(\text{SnPh}_3)_2(\mu\text{-H})_2$  (**2**) (20% yield) and  $\text{Ru}_3(\text{CO})_9(\text{SnPh}_3)_3(\mu\text{-H})_3$  (**6**), but the reaction of **5** with CO is slow and the yield of **6** is very low (4%). Fortunately, we have found that compound **6** can be prepared in a much better yield (44%) directly from the reaction of  $\text{Ru}_3(\text{CO})_{12}$  with  $\text{HSnPh}_3$  under a hydrogen atmosphere in heptane solvent at reflux for 90 min. Compound **6** was characterized by single crystal X-ray diffraction analysis. ORTEP diagrams of the molecular structure of **6** is shown in Fig. 4. In the solid state compound **6** crystallizes with three  $1/3$  molecules in the asymmetric unit. Each one lies on a threefold rotation axis. One of the molecules is disordered, see Section 2 above for details. Each molecule has crystallographic  $\text{C}_3$  symmetry. The  $\text{Ru}_3\text{Sn}_3$  core of the cluster has approximate  $\text{C}_{3\text{h}}$  symmetry. The cluster consists of a  $\text{Ru}_3$  triangle with three hydride-bridged Ru–Ru bonds. The Ru–Ru bond distances in **6** are similar in length to the hydride-bridged Ru–Ru bonds in **1**, **2** and **5**, Ru(1)–Ru(1 $^*$ ) = 3.1298(10) Å, Ru(2)–Ru(2 $^*$ ) = 3.1062(10) Å, Ru(3A)–Ru(3A $^*$ ) = 3.1351(16) Å. The Ru–Sn bond distances are also very similar to those found in **1**, **2** and **5**: Ru(1)–Sn(1) = 2.6897(8), Ru(2)–Sn(2) = 2.6892(7), Ru(3A)–Sn(3A) = 2.6833(13). Except for the disordered molecule, the hydrido ligands were located and refined Ru(1)–H(1) = 1.68(6) Å, Ru(2)–H(2) = 1.75(6) Å in the structural analysis. They are all equivalent and appear as a single resonance in the  $^1\text{H}$  NMR spectrum,  $\delta = -14.60$ . Compound **6** is structurally similar to the compound  $\text{Ru}_3(\text{CO})_9(\text{GePh}_3)_3(\mu\text{-H})_3$  that has been reported from the reaction of  $\text{Ru}_3(\text{CO})_{12}$  with  $\text{HGePh}_3$  [24].

When compound **2** was heated to reflux in benzene solution for 30 min, it was converted to the new compound **7** in 61% yield. An ORTEP diagram of the molecular structure of **7** is shown in Fig. 5.

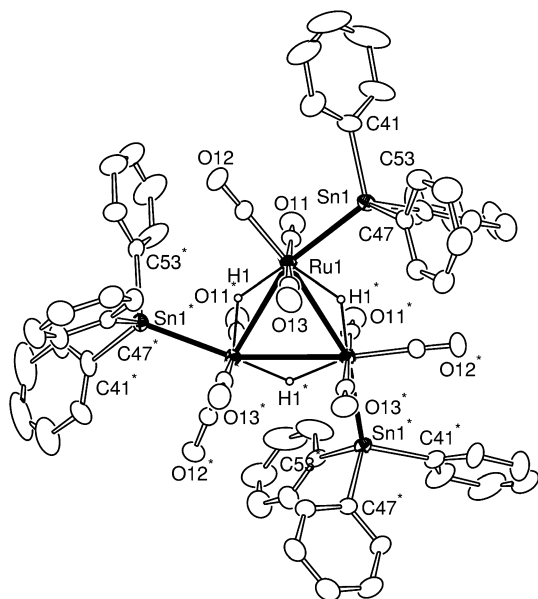


**Fig. 4.** An ORTEP diagram of the molecular structure of **6** showing 30% probability thermal ellipsoids. The hydrogen atoms are omitted for clarity. Selected interatomic bond distances (Å) and angles (°) are as follows: (molecule 1) Ru(1)–Ru(1) = 3.1298(10), Ru(1)–Sn(1) = 2.6897(8), Ru(1)–H(1) = 1.68(6), (molecule 2) Ru(2)–Ru(2) = 3.1062(10), Ru(2)–Sn(2) = 2.6892(7), Ru(2)–H(2) = 1.75(6), (molecule 3) Ru(3A)–Ru(3A) = 3.1351(16), Ru(3A)–Sn(3A) = 2.6833(13).

Compound **7** consists of a triangular cluster of three ruthenium atoms with two SnPh<sub>2</sub> ligands bridging adjacent Ru–Ru bonds. The third Ru–Ru bond contains a bridging CO ligand. The tin bridged Ru–Ru bond distances, Ru(1)–Ru(2) = 2.9963(5) Å, Ru(1)–Ru(3) = 2.9954(5) Å, are similar to the Ru–Ru bond distances found in the tris-SnPh<sub>2</sub> compound **8**, [12] and are significantly longer than the CO bridged Ru–Ru bond, Ru(2)–Ru(3) = 2.8520(5) Å. The Ru–Sn bond distances in **7**, Ru(1)–Sn(1) = 2.6593(5) Å, Ru(1)–

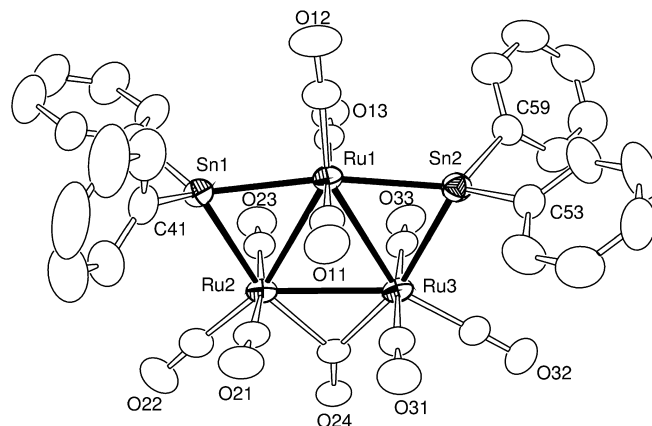


**Fig. 5.** An ORTEP diagram of the molecular structure of **7** showing 30% probability thermal ellipsoids. Selected interatomic bond distances (in Å) and angles (°) are as follows: Ru(1)–Ru(2) = 2.9963(5), Ru(1)–Ru(3) = 2.9954(5), Ru(2)–Ru(3) = 2.8520(5), Ru(1)–Sn(2) = 2.6377(5), Ru(1)–Sn(1) = 2.6593(5), Ru(2)–Sn(1) = 2.6547(5), Ru(3)–Sn(2) = 2.6847(5); Sn(2)–Ru(1)–Sn(1) = 168.825(17), Ru(2)–Sn(1)–Ru(1) = 68.645(13), Ru(1)–Sn(2)–Ru(3) = 68.489(13).

Sn(2) = 2.6377(5) Å, Ru(2)–Sn(1) = 2.6547(5) Å, Ru(3)–Sn(2) = 2.6847(5) Å, are similar to the Ru–Sn bond distances found in **8**. Each ruthenium atom also contains three linear terminal carbonyl ligands, two occupy axial sites perpendicular to the Ru<sub>3</sub> triangle and one lies in the plane of the Ru<sub>3</sub> triangle. Compound **7** was formed by the loss of two phenyl groups, one from each SnPh<sub>3</sub> ligand, and the two hydrido ligands. These ligands combined to form benzene which was confirmed by <sup>1</sup>H NMR spectroscopy. Compound **7** is structurally similar to its germanium homolog, Ru<sub>3</sub>(CO)<sub>10</sub>(μ-GePh<sub>2</sub>)<sub>2</sub>, which was obtained as a product of the thermal decomposition of the compound Ru<sub>3</sub>(CO)<sub>9</sub>(GePh<sub>3</sub>)<sub>3</sub>(μ-H)<sub>3</sub> [24].

To obtain an understanding of the metal–metal bonding in **7**, a Fenske–Hall molecular orbital analysis was performed. The metal–metal bonding in **7** is represented best by the contour diagrams of

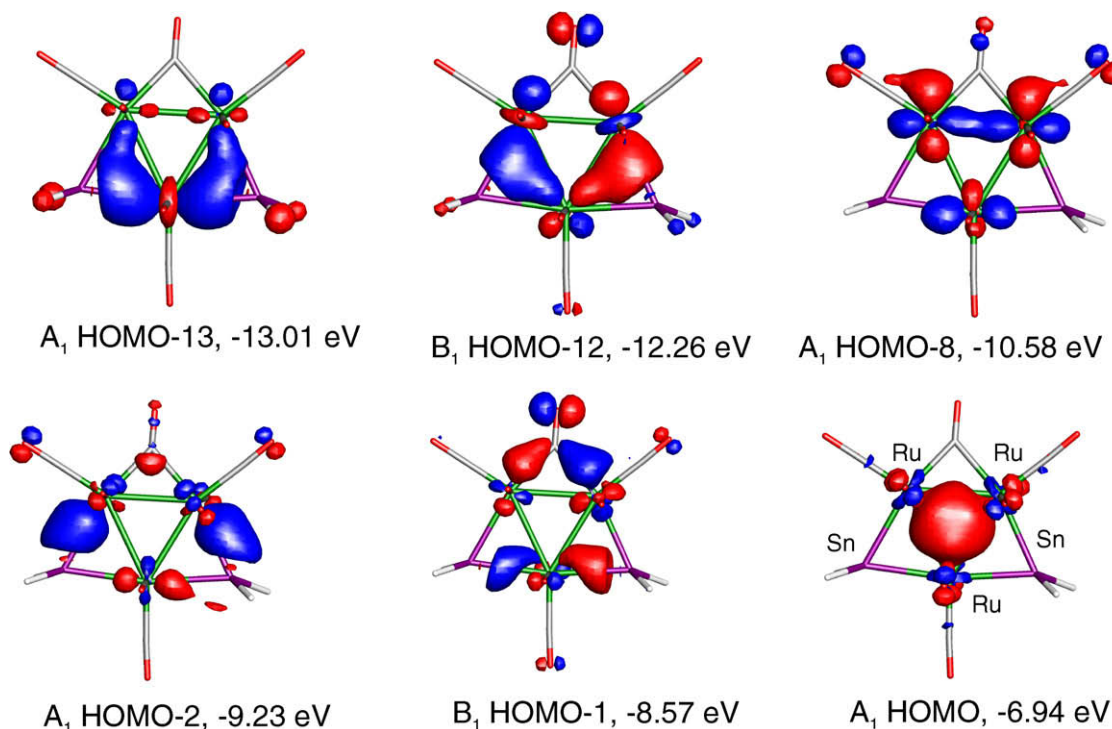


**Fig. 6.** Contour diagrams for the molecular orbitals that show the metal–metal bonding in **7**.

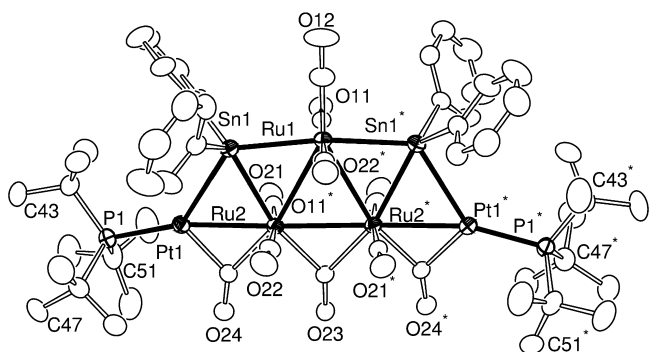


**Fig. 7.** ORTEP diagram of the molecular structure of **9** showing 30% probability thermal ellipsoids. The hydrogen atoms are omitted for clarity. Selected interatomic bond distances (in Å) each of the four independent molecules in the unit cell are as follows: Ru(1)–Ru(2) = 2.9622(6), Ru(1)–Sn(1) = 2.6819(3), Ru(2)–Sn(1) = 2.7157(5), Pt(1)–Sn(1) = 2.8328(4), Ru(2)–Pt(1) = 2.7319(4), Ru(2)–Ru(2') = 2.8449(7), Pt(1)–Pt(1) = 2.3035(12).

six molecular orbitals shown in Fig. 6. The Ru–Ru bonding is represented by the HOMO at  $-6.94$  eV and the HOMO–8 at  $-10.58$  eV. The bonding between the ruthenium atoms and the bridging tin atoms is best shown by the HOMO–1,  $-8.67$  eV, the HOMO–2 at  $-9.23$  eV, the HOMO–12 at  $-12.26$  eV and the HOMO–13, at  $-13.01$  eV, although the HOMO–1 and HOMO–12 also contain significant contributions from the bridging CO ligand.

When **6** was heated to reflux in octane solvent ( $125$  °C), it was converted into the known compound **8** in 85% yield by the elimination of three equivalents of benzene. Although **6** was not reported previously, it seems likely that this compound is an intermediate in the formation of **8** from the reaction of  $\text{Ru}_3(\text{CO})_{12}$  with  $\text{HSnPh}_3$  [12].

In previous work it was shown that it is possible to add  $\text{Pt}(\text{PBU}_3)_2$  groupings both to Ru–Sn bonds, Eqs. (5) [12] and (6) [11] and also to Ru–Ru bonds [25]. Accordingly, we also investigated the reaction of **7** with  $\text{Pt}(\text{PBU}_3)_2$ . The compound  $\text{Pt}_2\text{Ru}_3(\text{CO})_{10}(\text{PBU}_3)_2(\mu_3\text{-SnPh}_2)_2$  (**9**) was obtained in 59% yield from the reaction of **7** with  $\text{Pt}(\text{PBU}_3)_2$  at room temperature in 65 min. An ORTEP diagram of the molecular structure of **9** is shown in Fig. 7. In the solid state the molecule lies on a two-fold rotation axis. The molecule is structurally similar to **7**

except that it contains two additional  $\text{Pt}(\text{PBU}_3)_2$  groupings that were added as bridges across two of the Ru–Sn bonds as shown in Fig. 7. The bridging  $\text{SnPh}_2$  ligands in **7** are converted into triply bridging  $\text{SnPh}_2$  ligands in **9** upon the attachment of the  $\text{Pt}(\text{PBU}_3)_2$  groups. The Ru–Ru bonds in **9** are slightly shorter than those in **7**: Ru(1)–Ru(2) =  $2.9622(6)$  Å and Ru(2)–Ru(2') =  $2.8449(7)$  Å. The platinum-bridged Ru–Sn bond distance, Ru(2)–Sn(1) =  $2.7157(5)$  Å, has increased in length (approx.  $0.07$  Å) compared to those in **7**. The unbridged Ru–Sn bond has also increased in length, but to a much smaller extent (approx.  $0.02$  Å), Ru(1)–Sn(1) =  $2.6819(3)$  Å. Two of the terminal CO ligands in **7** have shifted to bridging sites, one across each of the new Pt–Ru bonds. A similar CO shift was observed when  $\text{Pt}(\text{PBU}_3)_2$  groups were added to the Ru–Sn bonds in the related compounds  $\text{Pt}_2\text{Ru}_3(\text{CO})_{10}(\text{PBU}_3)_2(\mu_3\text{-SnPh}_2)_2$ , **10–12**,  $n = 1–3$  [12]. The Ru–Pt bond distance in **9**, Ru(2)–Pt(1) =  $2.7319(4)$  Å is very similar to those in **10–12**. However, the Pt–Sn distance, Pt(1)–Sn(1) =  $2.8328(4)$  Å, in **9** is slightly, but significantly longer, than those in the compounds **10–12**, range =  $2.7433(7)–2.7922(15)$  Å [12]. Compound **9** was also obtained from the reaction of **1** with  $\text{Pt}(\text{PBU}_3)_2$  but the yield was much lower, 7%. The low yield may be due to the requirement to add a CO ligand which must be scavenged from the reaction-mixture in order to form **9**.

In previous studies it has been shown that the bonding of  $\text{Pt}(\text{PBU}_3)_2$  groupings to homo- and heteronuclear metal–metal bonds can be quite complex particularly when more than one  $\text{Pt}(\text{PBU}_3)_2$  grouping is involved [8,12,26]. To develop a better understanding of the metal–metal bonding in **9** and to compare it with that in **7**, a Fenske–Hall molecular orbital analysis was performed. Contour diagrams of the molecular orbitals that show the interactions of the two platinum atoms with the  $\text{Ru}_3\text{Sn}_2$  core of the cluster are shown in Fig. 8. The platinum atoms interact with the ruthenium–tin bonds represented by the HOMO–2 orbital in **7** to create the HOMO–2 orbital in **9**. The platinum–ruthenium bonding is best shown by the three orbitals: the symmetric HOMO–2,  $-7.71$  eV, the antisymmetric HOMO–12  $-9.69$  eV and the symmetric HOMO–13,  $-9.72$  eV. The tin atoms are formally 5-coordinate, but the platinum–tin interactions are weak and the only orbital that exhibits any significant Pt–Sn interactions is the antisymmetric HOMO–22 at  $-11.51$  eV. As in **7**, the HOMO in **9** at  $-6.09$  eV is predominantly Ru–Ru bonding and the HOMO–23 at  $-11.87$  eV is predominantly Ru–Sn bonding as it was in the HOMO–13 in **7**.

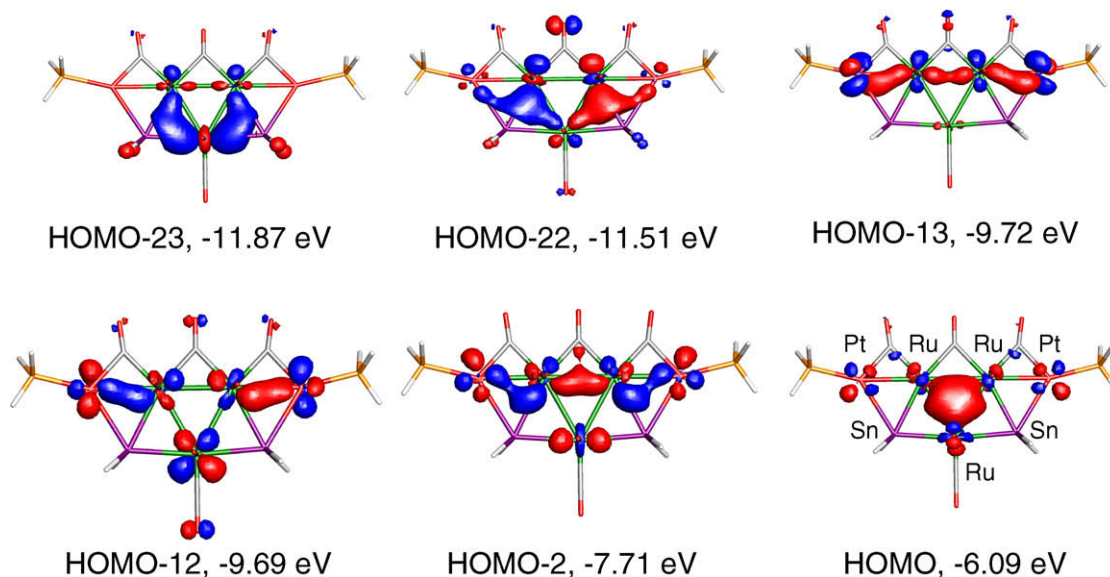


**Fig. 8.** Contour diagrams of the FH molecular orbitals in **9** that show the metal–metal bonding.





## Acknowledgements

This research was supported by the National Science Foundation under Grant No. CHE-0743190. This report is dedicated to the memory of Professor F. Albert Cotton.

## Appendix A. Supplementary material

CCDC 698764, 698763, 698765, 698766, 698767 and 698768 contains the supplementary crystallographic data for **1**, **2**, **5**, **6**, **7**, **8** and **9**. These data can be obtained free of charge from The Cambridge Crystallographic Data Centre via [www.ccdc.cam.ac.uk/data\\_request/cif](http://www.ccdc.cam.ac.uk/data_request/cif). Supplementary data associated with this article can be found, in the online version, at [doi:10.1016/j.jorganchem.2008.08.033](https://doi.org/10.1016/j.jorganchem.2008.08.033).

## References

- [1] (a) R. Burch, L.C. Garla, *J. Catal.* **71** (1981) 360–372;  
(b) R. Srinivasan, B.H. Davis, *Platinum Met. Rev.* **36** (1992) 151;  
(c) R.D. Cortright, J.A. Dumesic, *J. Catal.* **148** (1994) 771–778;  
(d) R.D. Cortright, J.A. Dumesic, *Appl. Catal. A Gen.* **129** (1995) 101–115;  
(e) R.D. Cortright, J.A. Dumesic, *J. Catal.* **157** (1995) 576–583;  
(f) T. Mallat, A. Baiker, *Appl. Catal. A Gen.* **200** (2000) 3–22;  
(g) K. Yoshikawa, Y. Iwasawa, *J. Mol. Catal.* **100** (1995) 115–127;  
(h) V. Gerstosio, C.C. Santini, M. Taoufik, F. Bayard, J.-M. Basset, J. Buendia, M. Vivat, *J. Catal.* **199** (2001) 1–8;  
(i) J. Ruiz-Martinez, A. Sepulveda-Escribano, J.A. Anderson, F. Rodriguez-Reinoso, *Catal. Today* **123** (2007) 235–244.
- [2] R.D. Adams, E.M. Boswell, B. Captain, A.B. Hungria, P.A. Midgley, R. Raja, J.M. Thomas, *Angew. Chem., Int. Ed.* **46** (2007) 8182–8185.
- [3] A.B. Hungria, R. Raja, R.D. Adams, B. Captain, J.M. Thomas, P.A. Midgley, V. Golvenko, B.F.G. Johnson, *Angew. Chem., Int. Ed.* **45** (2006) 4782–4785.
- [4] J.M. Thomas, R.D. Adams, E.M. Boswell, B. Captain, H. Grönbeck, R. Raja, *Faraday Disc.* **138** (2008) 301–315.
- [5] R.D. Adams, D.A. Blom, B. Captain, R. Raja, J.M. Thomas, E. Trufan, *Langmuir* **24** (2008) 9223–9226.
- [6] R.D. Adams, B. Captain, W. Fu, M.D. Smith, *Inorg. Chem.* **41** (2002) 2302–2303.
- [7] R.D. Adams, B. Captain, J.L. Smith Jr, M.B. Hall, C.E. Webster, *Inorg. Chem.* **43** (2004) 7576–7578.
- [8] R.D. Adams, B. Captain, R.H. Herber, M. Johansson, I. Nowik, J.L. Smith Jr, M.D. Smith, *Inorg. Chem.* **44** (2005) 6346–6358.
- [9] R.D. Adams, B. Captain, L. Zhu, *Organometallics* **25** (2006) 2049–2054.
- [10] R.D. Adams, B. Captain, L. Zhu, *Organometallics* **25** (2006) 4183–4187.
- [11] R.D. Adams, E. Trufan, *Organometallics*, ASAP, 2008.
- [12] R.D. Adams, B. Captain, M.B. Hall, E. Trufan, X. Yang, *J. Am. Chem. Soc.* **129** (2007) 12328–12340.
- [13] J.D. Cotton, S.A.R. Knox, F.G.A. Stone, *Chem. Commun.* (1967) 965–966.
- [14] K. Burgess, C. Guerin, B.F.G. Johnson, J. Lewis, *J. Organomet. Chem.* **295** (1985) C3–C6.
- [15] G.A. Foulds, B.F.G. Johnson, J. Lewis, *J. Organomet. Chem.* **296** (1985) 147–153.
- [16] R.D. Adams, B. Captain, E. Trufan, L. Zhu, *J. Am. Chem. Soc.* **129** (2007) 7545–7556.
- [17] SAINT+ Version 6.2a, Bruker Analytical X-Ray System, Inc., Madison, Wisconsin, USA, 2001.
- [18] G.M. Sheldrick, SHELXL Version 6.1, Bruker Analytical X-Ray Systems, Inc., Madison, Wisconsin, USA, 1997.
- [19] (a) M.B. Hall, R.F. Fenske, *Inorg. Chem.* **11** (1972) 768–775;  
(b) C.E. Webster, M.B. Hall, in: C. Dykstra (Ed.), *Theory and Applications of Computational Chemistry: The First Forty Years*, Elsevier, Amsterdam, 2005, pp. 1143–1165 (Chapter 40).
- [20] J. Manson, C.E. Webster, L.M. Pérez, M.B. Hall, JIMP2, Development Version 0.1.v117 (built for Windows PC and Redhat Linux), Department of Chemistry, Texas A&M University, College Station, TX, <<http://www.chem.tamu.edu/jimp2/index.html>> (accessed July 2004).
- [21] MOPLLOT2 for orbital and density plots from linear combinations of SLATER or GAUSSIAN type orbitals, Version 2.0, D.L. Lichtenberger, Department of Chemistry, University of Arizona, Tucson, AZ, 1993.
- [22] M.R. Churchill, F.J. Hollander, J.P. Hutchinson, *Inorg. Chem.* **16** (1977) 2655.
- [23] (a) R. Bau, M.H. Drabnis, *Inorg. Chim. Acta* **259** (1997) 27–50;  
(b) R.G. Teller, R. Bau, *Struct. Bond.* **41** (1981) 1–82.
- [24] R.D. Adams, B. Captain, E. Trufan, *J. Clust. Sci.* **18** (2007) 642–659.
- [25] R.D. Adams, E.M. Boswell, B. Captain, L. Zhu, *J. Clust. Sci.* **19** (2008) 121–132.
- [26] R.D. Adams, B. Captain, W. Fu, M.B. Hall, J. Manson, M.D. Smith, C.E. Webster, *J. Am. Chem. Soc.* **126** (2004) 5253–5267.